Dynamics of the surface layer in cyanobiphenyl-aerosil nanocomposites with a high silica density

S. Frunza Corresponding author[a]; L. Frunza[a]; M. Tintaru[a]; I. Enache[a]; T. Beica[a]; A. Schönhals Corresponding author[b]

[a] National Institute of Materials Physics, R-77125 Bucharest-Magurele, Romania [b] Federal Institute of Materials Research and Testing, D-12205 Berlin, Germany

PLEASE SCROLL DOWN FOR ARTICLE

Dynamics of the surface layer in cyanobiphenyl–aerosil nanocomposites with a high silica density

S. FRUNZA*, L. FRUNZA, M. TINTARU, I. ENACHE, T. BEICA

National Institute of Materials Physics, R-77125 Bucharest-Magurele, Romania

and A. SCHÖNHALS*

Federal Institute of Materials Research and Testing, D-12205 Berlin, Germany

Composites were prepared from an aerosil and 4-n-alkyl-4′cyanobiphenyls with five to eight carbon atoms in the alkyl chain. Their high silica density of ~ 7 g aerosil in $1\,cm^3$ of liquid crystal (LC) allows the observation of the behaviour of a thin cyanobiphenyl layer (having nearly a monolayer structure) on the silica particles. The systems are investigated by dielectric spectroscopy (10^{-2}–$10^9\,Hz$) in a large temperature range (220–370 K). All the composites show a (main) relaxation process at frequencies much lower than the processes observed for the bulk LC that was assigned to the dynamics of the molecules in the surface layer. The temperature dependence of its characteristic frequencies obeys the Vogel–Fulcher–Tammann law, which is found to be typical for glass-forming liquids. The quasi two-dimensional character of the glass transition in the surface layer is discussed for the first time. At the nematic-to-isotropic transition temperature of the bulk, the composites show a continuous decrease of the characteristic frequencies as a function of the alkyl chain length, while the bulk LCs show the well known odd–even behaviour. The magnitude and temperature dependence of the slow relaxation process in the composites (molecules on an outer surface) agree with those of the same molecules confined to the nanopores of molecular sieves (internal surface).

1. Introduction

Liquid crystals in complex geometries such as networks, porous materials or polymers [1] have been intensively studied in order to observe the effects of finite size, of the surface as well as of the random disorder. Related systems such as composites containing LCs and aerosil particles have also attracted special particular interest from both technological and theoretical points of view since these systems allow for the induction of a transparent state under the influence of an electric field that remains stable if the field is removed [2–5]. Moreover a random disorder might be introduced in a controlled manner so that the properties vary continuously with the aerosil concentration [6–12]. Cyanobiphenyls (CBs) were often used as the organic components of such composites, but other LCs have also been considered [13].

Most of the investigations were carried out for octylcyanobiphenyl-containing composites with low silica densities, ρ_s (g silica per $1\,cm^3$ of LC) ranging

from 0.005 to $0.825\,g\,cm^{-3}$. But recently, high values of silica densities (up to $10\,g\,cm^{-3}$) were achieved for the first time in order to investigate the properties of a surface layer formed by the CB molecules onto the silica particles separately from the properties of the bulk LC [14]. The relaxation characteristics of the bulk LC can be observed for samples with low silica densities. In addition to the bulk-like relaxation, a slow relaxation process was detected for all the samples, which was assigned to the layer of CB molecules adsorbed on the surface of the silica particles. With increasing silica concentration the latter process is better resolved and for high silica concentrations it is the only relaxation process that can be detected. It is noteworthy that this relaxation process can be observed even at temperatures at which the bulk is in the crystalline state.

This paper compares results on the surface layer obtained by broadband dielectric spectroscopy (10^{-2}–$10^9\,Hz$) for composite systems consisting of aerosil nanoparticles mixed with liquid crystals from the 4-n-alkyl-4′cynobiphenyl series with five to eight carbon atoms in the alkyl chain (5CB–8CB), having the
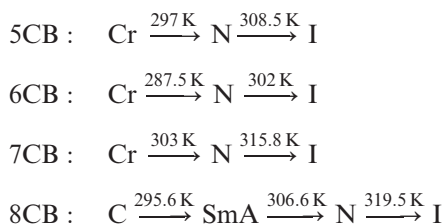
*Author for correspondence;
e-mail: ifrunza@infim.ro; andreas.schoenhals@bam.de

same high silica density ($\rho_s = 7 \, \text{g cm}^{-3}$). The temperature range of the measurements (220–370 K) covers not only the range of phase transitions characteristic for the corresponding bulk LCs but also extends considerably into the crystalline and in the isotropic states.

2.   Experimental

The liquid crystals (Aldrich) used in these experiments are well known single component materials. The phase transition temperatures, where Cr symbolizes, the crystalline, SmA the smectic A, N the nematic and I the isotropic state, are:

$$5CB: \quad Cr \xrightarrow{297 \, K} N \xrightarrow{308.5 \, K} I$$

$$6CB: \quad Cr \xrightarrow{287.5 \, K} N \xrightarrow{302 \, K} I$$

$$7CB: \quad Cr \xrightarrow{303 \, K} N \xrightarrow{315.8 \, K} I$$

$$8CB: \quad C \xrightarrow{295.6 \, K} SmA \xrightarrow{306.6 \, K} N \xrightarrow{319.5 \, K} I$$

The hydrophilic aerosil A_{380} (type 380, from Degussa-Hüls) with a specific surface BET area of $380 \, \text{m}^2 \, \text{g}^{-1}$ consists of silica spheres of 7 nm diameter, covered by hydroxyl groups. It was used after drying under vacuum at ~ 500 K for at least 12 h. Aerosil–LC nanocomposites were prepared applying a solution route according to the literature [5, 6], by mixing the aerosil particles with a solution of the corresponding CB in carbon tetrachloride. The solvent was subsequently removed under a mild vacuum at 348 K for 20 h. Its complete removal was checked by blank experiments. This method allows us to achieve high values of ρ_s.

In order to monitor the CB amount, silica densities of the samples were estimated by thermogravimetry, using a TG-DTA 92 equipment (Setaram), under a dry airflow, at a heating rate of $10 \, \text{K min}^{-1}$. Vibrational spectra were recorded with a Nicolet Magna 550 FTIR spectrometer on thin self-supported pellets. The spectra were analysed by fitting Gaussian profiles to the data. The equipment to measure the complex dielectric function $\varepsilon^*(f) = \varepsilon'(f) - i\varepsilon''(f)$ ($f =$ frequency, $\varepsilon' =$ real part, $\varepsilon'' =$ imaginary part) has been described in detail elsewhere [15] and the method to analyse and separate relaxation processes according to the model function of Havriliak–Negami (HN-function) has also been given [16]. The HN-function reads:

$$\varepsilon^*(f) - \varepsilon_\infty = \frac{\Delta\varepsilon}{\left[1 + (if/f_0)^\beta\right]^\gamma} \quad (1)$$

where f_0 is a characteristic frequency related to the

frequency of maximal loss f_p, and ε_∞ describes the values of the real part ε' for $f \gg f_0$. β and γ are fractional form parameters ($0 < \beta \leqslant 1$ and $0 < \beta\gamma \leqslant 1$) characterizing the shape of the relaxation time spectra. $\Delta\varepsilon$ denotes the dielectric strength, which is proportional to the effective dipole moment and to the density of the fluctuating dipoles. Conductive effects are treated in the usual way by adding a conductivity contribution $\sigma_0/[\varepsilon_0(2\pi f)^s]$ to the dielectric loss where σ_0 is related to the d.c. conductivity of the sample and ε_0 is the dielectric permittivity of vacuum ($\varepsilon_0 = 8.854 \times 10^{-12} \, \text{As V}^{-1} \text{m}^{-1}$). The parameter s ($0 < s \leqslant 1$) describes for $s < 1$ non-Ohmic effects in the conductivity, for details see [16].

The temperature of the isothermal dielectric measurements was varied from 220 to 373 K in order to cover temperatures well into the crystalline state of the LCs, all phase transition temperatures, and high temperatures into the isotropic state of the bulk LCs. The results obtained for the bulk LC were compared with the spectra of the nanocomposites where special attention was paid to the surface layer covering the aerosil particles. The temperature dependence of the relaxation rates f_p is analysed and discussed in detail.

3.   Results and discussions

It is well known that aerosil particles are covered by surface hydroxyl groups and consequently, they can hydrogen bond to each other in a suitable medium forming a gel [6]. Since in the composites investigated the silica density is higher than a certain threshold, the gel is 'rigid' and similar to an aerogel. Aerosil-based systems have a hierarchical structure consisting of different length scales. It was suggested that individual 7 nm aerosil particles fused together during the manufacturing process to larger primary particles of *ca.* 20 nm [6]. These primary particles accumulate to 440 nm aggregates and even further, these aggregates forming macroscopic agglomerates. Therefore, it is expected that composite samples with high silica densities consist of aggregates and agglomerates formed by primary silica particles. This is also indicated by AFM images [14] in agreement with the literature.

The loading of the silica system with CB molecules was checked by TGA experiments, and similar loadings expressed by similar silica densities between 7.16 and 7.60 are found. In accord with previous estimations [14], for this amount of CB molecules a monolayer with high packing density can be formed, assuming a perpendicular orientation of the molecules to the surface of the aerosil particles. To illustrate this, for a van der Waals molecular surface of 8CB of $0.2 \, \text{nm}^2$, and a medium size of aerosil particles of 50 nm, an 8CB monolayer is attained for $\rho_s = 7.5 \, \text{g cm}^{-3}$. The other cyanobiphenyls used have a similar molecular size and

weight as 8CB; therefore a similar silica density is expected to lead to the corresponding monolayer.

3.1. *IR spectroscopic features of the surface layer*

The influence of the surface layer on the composite properties depends on the intrinsic properties of the two components, and on the type and strength of their interactions. The large surface-to-volume ratio of the dispersions studied leads to a considerable contribution from molecules of the LC surface layer to the spectra (and to other composite properties). Therefore, information on interactions between the components in this surface layer can be obtained from the IR spectra.

Strong anchoring at the particle surface by hydrogen bonds between the cyano groups of the 8CB molecules and the hydroxyl groups of the silica surface has been demonstrated by FTIR measurements [17]. Similar features are shown in the spectra of the composites containing the other CBs: figure 1 gives a representative spectrum of the composite based on 7CB in the wavenumber region in which the aerosil is transparent to IR radiation. The spectrum of the composite is compared with that of pure 7CB and of the unloaded aerosil.

The spectra for the composites are complex and contain peaks due to both components. Some of the peaks are changed compared with the pure components, the observed changes reflecting interactions in different microenvironments. Some peaks can be identified as being due to 7CB, such as: at frequencies 3026–3073 cm^{-1}, $C_{arom}H$ stretch, between 2956 and 2857 cm^{-1}, CH_3 and CH_2 asymmetrical and symmetrical stretches; at 2226 cm^{-1}, CN stretch, at 1606 and 1494 cm^{-1}, $C_{arom}C_{arom}$ stretch, at 1460, 1397 and 1378 cm^{-1}, alkyl deformation; and at 1285 cm^{-1}, CC biphenyl bridge stretch. The assignments of the
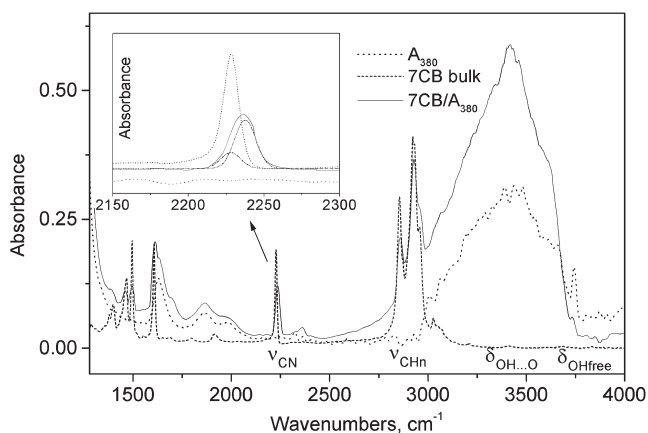

Figure 1. IR spectrum of 7CB/A$_{380}$ composite in comparison with the spectrum of free 7CB and of aerosil A$_{380}$.

observed LC peaks are taken from the literature for bulk 8CB and related compounds [17]. Among these, the CN stretch seems to be the only one to be truly due to a vibration of a localized group and is consequently suitable to be decomposed into components for further discussion.

The spectral interval shown in figure 1 does not include the regions in which the main peaks characteristic of the aerosil appear, but some weak peaks can be assigned to overtones and combination tones of the fundamental vibrations of silica tetrahedra, such as those at 1875, 1975 and *ca.* 1640 cm^{-1}; the latter overlays a water deformation peak. In addition, hydroxyl groups attached to silica surfaces give a broad band at 3400 cm^{-1} due to the stretching vibrations of those groups which are hydrogen-bonded, while the peak at 3750 cm^{-1} corresponds to free hydroxyl groups. Its intensity decreases for the composites in comparison with the pure aerosil, probably due to interaction with the CB molecules.

The broad asymmetrical absorption peak observed in the nitrile stretching region results from the overlapping of peaks due to two/three species carrying cyano groups: some of them form hydrogen bonds with free silanols and others are sterically hindered to form hydrogen bonds with the substrate. This range is magnified in the inset of figure 1 and includes the decomposition into Gaussian components. Nitrile interaction with different adsorption sites has been discussed in detail in the literature. Three species of nitrile-containing CB molecules coated on silica materials were found [17]: in the 'LC' state, in a randomized state and in the hydrogen-bonded state, in the sequence of increasing frequency (2226, *ca.* 2235 and 2240 cm^{-1}, respectively). Composites with a silica density of 7 g cm^{-3} show mostly two species: those responsible for the peak at 2226 cm^{-1} and that hydrogen-bonded (responsible for the peak at 2240 cm^{-1}). Moreover, the peak at the lowest frequency is larger than for the bulk (7CB in figure 1). The peak broadening is mainly due to interactions between 7CB molecules and the silica surface, in addition to the hydrogen bonding.

It is interesting to note that the peak due to hydrogen-bonded species represents the largest contribution to the asymmetric CN stretch peak. Its integrated intensity is 66–70% for all composites. Because the molar absorptivity is not available in the literature for hydrogen-bonded cyano groups, or for these groups in comparison with that of the free groups, the high relative value of the integrated area of the peak due to these hydrogen bonded species indicates that a large number of CB molecules (approximately constant for all investigated composites) are involved in these bonds. Most probably, these

hydrogen bonds involve all available hydroxyl groups. In fact, 1 nm² of aerosil surface can offer up to three hydroxyl groups [18] and can accommodate five CB molecules [14]. At most 60% of these CB molecules on the aerosil surface can therefore form hydrogen bonds with the surface, a percentage close to those found by the band shape analysis of the CN stretch peak.

3.2. *Dielectric relaxation spectra of bulk cyanobiphenyls*

The dielectric properties of cyanobiphenyls have been investigated for many years. During the last decade dielectric measurements were performed under special conditions (unaligned samples, enlarged frequency/temperature interval, high pressure) or were related to the properties of complex composite systems [19–22].

Liquid crystals are anisotropic materials; therefore the dielectric function must be described by a tensor, which for uniaxial nematic phases has two main components $\varepsilon_\parallel^*$ and $\varepsilon_\perp^*(f)$, parallel and perpendicular to the nematic director, respectively. The theoretical background of the dielectric relaxation is outlined briefly in [22]; for a more detailed discussion see, for example, [23]. One has to consider that each mesogenic unit has two components of the molecular dipole vector, longitudinal and transverse to its long axis. The dielectric response is due to correlation functions of the polarization fluctuations parallel and perpendicular to the nematic director. In a semi-microscopic treatment the measured dielectric functions parallel $\varepsilon_\parallel^*(f)$ and perpendicular $\varepsilon_\perp^*(f)$ to the director comprise different weighted sums of the four underlying relaxation modes depending on the macroscopic orientation of the sample. The relaxation mode at the lowest frequencies is due to rotational fluctuations of the molecule around the short axis. This process mainly determines $\varepsilon_\parallel^*(f)$. The other three relaxation modes (different tumbling modes of the molecules around their long axis) have nearly the same relaxation rate and form one broad relaxation process, which is mainly related to $\varepsilon_\perp^*(f)$; it is observed at higher frequencies than the former process. Newer theories predict one more movement, on a cone around the director [24].

According to the outlined theoretical approach the temperature dependence of the relaxation should obey the Arrhenius law:

$$f_p = f_\infty \exp\left(-\frac{E_A}{k_B T}\right) \tag{2}$$

where E_A is the activation energy, f_∞ is the pre-exponential factor, k_B is Boltzman's constant and T is temperature. This is found for a limited temperature

regime [19–22]. However, careful measurements performed over a large temperature interval, especially in the isotropic state, and a more detailed analysis have shown that the temperature dependence of the relaxation rates can be better described by the Vogel–Fulcher–Tammann (VFT) law:

$$\log f_p = \log f_\infty - \frac{A}{T - T_0} \tag{3}$$

where A is a constant and T_0 is the so-called Vogel temperature [22]. Deviations from the Arrhenius-like dependence in the temperature range of the mesophases have already been reported [25–27] for CBs and other nematics.

All bulk CBs were studied in the unaligned state because this corresponds to the situation in the composites. For example, in figure 2 the dielectric loss for an unaligned 6CB sample is given versus frequency and temperature. In the liquid crystalline state one main relaxation process is detected at lower frequencies and a shoulder at higher frequencies. According to the theory of the dielectric relaxation of low molar mass liquid crystals these processes are assigned to the tensorial components of the complex dielectric function parallel and perpendicular to the director [22]. According to this theoretical approach the process at lower frequencies is due to rotational fluctuations of the molecule around the short axis.

To analyse the spectra in the liquid crystalline state two HN-functions were fitted to the data (figure 3). Above the clearing temperature the two processes collapse into one broadened relaxation, and one
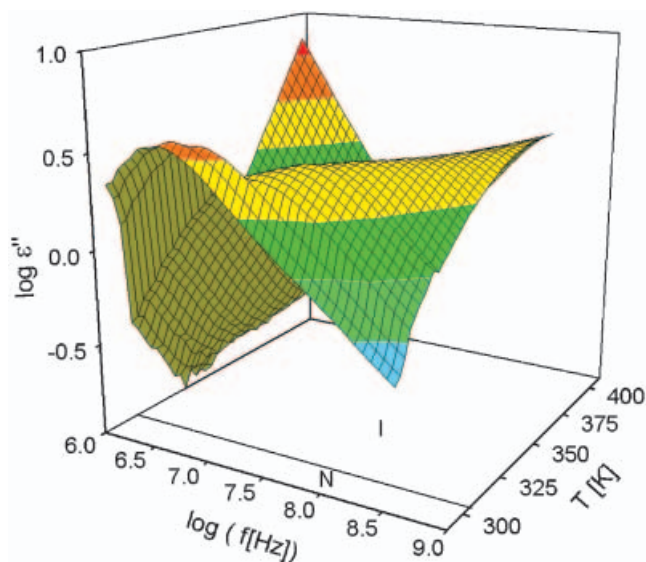

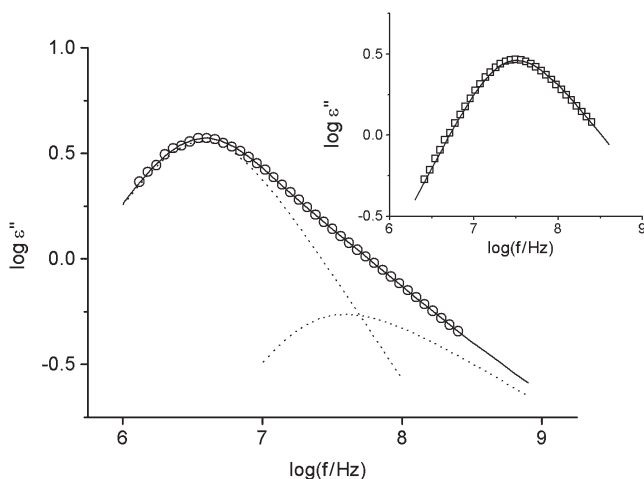Figure 2. Dielectric loss vs. frequency and temperature of bulk 6CB.

Figure 3. Dielectric loss vs. frequency for bulk 6CB at $T = 298.7$ K in the nematic phase. The solid line is a fit of two HN-functions to the data. The dotted lines are the HN-contributions of the two processes to the whole dielectric loss. The inset shows the dielectric loss for 6CB at $T = 319.7$ K in the isotropic state. The line is a fit of one HN-function to the data.

Figure 4. Relaxation rates for bulk CBs vs. inverse temperature for the δ-relaxation process: squares = 8CB, down-triangles = 7CB, up-triangles = 6CB, circles = 5CB. The dashed line is a fit of the Arrhenius equation to the data of 6CB ($\log(f_\infty/\text{Hz}) = 13.1$, $E_A = 34.4$ kJ mol^{-1}) which shows that the data are not adequately described by this equation. The inset gives $(\Delta \log f_p / \Delta T)^{-1/2}$ vs. T for all CB molecules in the isotropic state. The symbols are the same as in the main figure. The line is a linear regression to the data of 6CB.

HN-function is used to describe the dielectric spectra (inset of figure 3).

In the following discussion, particular attention is paid to the low frequency process. Due to the high dipole moment of the cyano group, the dielectric strength of this relaxation processes is high for bulk CBs. Thus, the dielectric behaviours of the LCs in the bulk can be easily compared. In addition, this relaxation process should be the main motional process observed for the composites. In figure 4 the characteristic frequencies determined for the low frequency process of bulk CBs are given versus inverse temperature. These frequencies are grouped in a rather narrow range, particularly in the temperature interval close to the crystalline state.

The characteristic frequency at a temperature in the vicinity of the N–I transition is plotted in figure 5 as function of the number of carbon atoms in the alkyl chain. As with many other properties (nematic-to-isotropic transition temperature, dielectric strength, the angle between the net dipole moment and the symmetry axis of the molecules, retardation factors, nematic potential, order parameter, the activation energies) of CB and other homologous series of liquid crystals, these frequencies alternate with the length of the alkyl chain (odd–even effect) [28]. A qualitative explanation of this effect starts by considering the molecular structure and the different angles formed with the molecular long axis by the carbon atoms: even-numbered atoms form larger angles than odd-numbered atoms, which lie along the long axis.
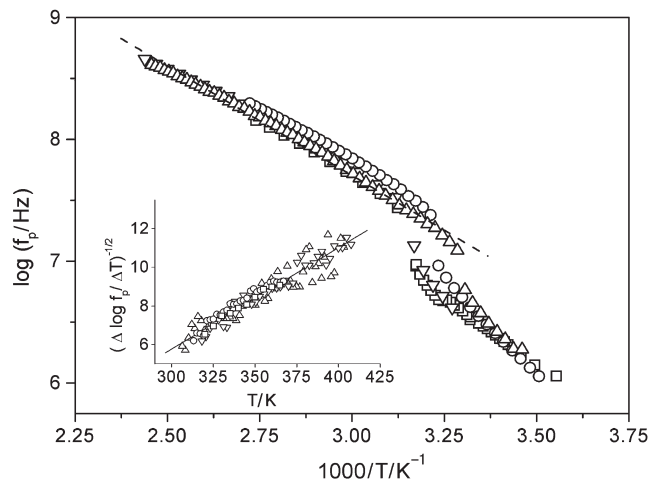
The end groups either enhance the molecular anisotropy and hence the molecular order, or have an opposite effect. As the chains lengthen, their flexibility increases and the alternation is less pronounced [29].

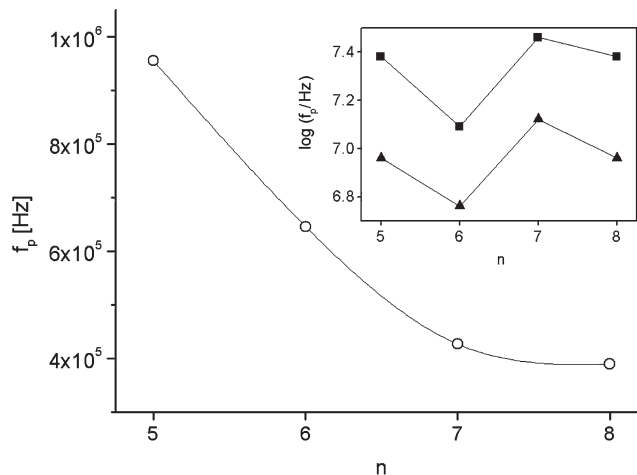Figure 5. Dependence of the relaxation rate on the number of carbon atoms in the alkyl chain n for the relaxation process assigned to the surface layer in the composites at a temperature corresponding to the N-I transition temperature of the bulk. The inset shows the same for bulk CBs in the isotropic state (square) at T_{NI+3} and in the nematic state (triangle) at T_{NI-3}. All lines in this figure are guides for the eyes.

The decrease of the antiparallel correlation in the isotropic phase at the transition temperature has also been suggested to contribute to the odd–even effect [30]. Going from the nematic to the isotropic phase, close to T_{NI} an odd–even effect is still observed in the isotropic range. This might indicate that a nematic-like ordering on a localized scale is present [29] at temperatures even higher than T_{NI}.

The data in the isotropic state can be only approximately described by an Arrhenius law (see the dotted line in figure 4). A more detailed analysis of the temperature dependence of the relaxation can be made by applying a derivative technique [22]. For the VFT equation one gets

$$\left(\frac{d \log f_p}{dT}\right)^{-1/2} = A^{-1/2}(T - T_0). \tag{4}$$

Thus a plot of $(d \log f_p / dT)^{-1/2}$ as a function of the temperature should give a straight line for a temperature dependence according to the VFT equation. The inset of figure 4 shows that the data can be well described by that relationship where for the homologous series quite similar values of the parameter A and T_0 are obtained. Therefore the differences in the absolute values of the relaxation rates (see inset of figure 5) must be attributed to differences in the prefactor f_∞.

3.3. *Cyanobiphenyls in composite systems*

CB molecules interact rather strongly with the silica surface, leading to a surface layer with a structure different from the bulk CB. Thus, the strong anchoring of the CB molecules implies a surface-induced order of these molecules resulting in a local para-nematic state. This was indicated by investigations of LCs confined to pores [19–22, 31–33] and for 8CB–aerosil composites in a large range of silica density [14]. The surface-induced order persists also in the temperature range corresponding to the isotropic bulk state, but decreases with increasing distance from the surface. Therefore it was expected that the molecular dynamics of the surface layer would be different from those of bulk CBs both in the liquid crystalline and in the isotropic state.

In figure 6, a plot of dielectric loss ε'' versus frequency is shown for aerosil composites based on 8CB, as representative spectra for the studied homologous series in the low frequency region, at temperatures where the bulk system is in the crystalline state, and hence no relaxation process can be observed at these temperatures for bulk CB. However, for the composites a relaxation process indicated by a peak in ε'' is visible in this frequency and temperature region. Its characteristic frequency increases with increasing
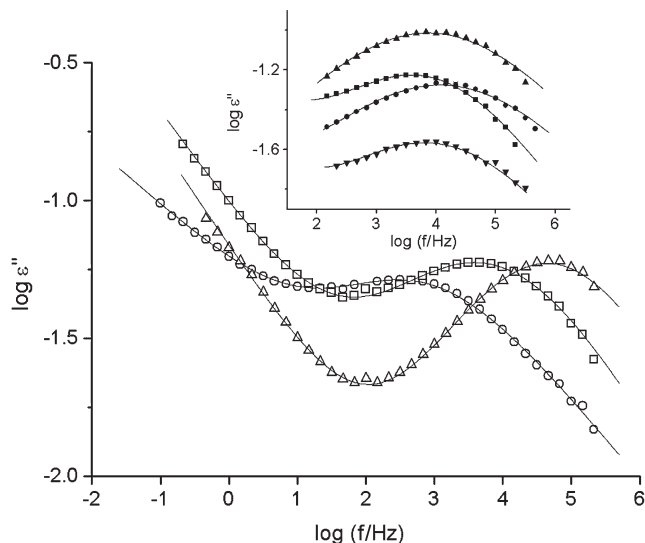

Figure 6.   Dielectric loss vs. frequency of 8CB/A$_{380}$ composites for different temperatures: circles $T = 245$ K, squares $T = 263.2$ K, triangles $T = 293.8$ K. The lines are fits of the HN-function to the data including a conductivity contribution. The inset gives the dielectric loss vs. frequency for A$_{380}$ composites with different CBs: squares 8CB at $T = 263.2$ K, down-triangles 7CB at $T = 265.6$ K; up-triangles 6CB at $T = 264.2$ K, circles 5CB at $T = 264.0$ K. The lines are fits of the HN-function to the data including a conductivity contribution.

temperature as expected (see figure 6) but its relaxation rate is lower by orders of magnitude than the relaxation rates for bulk CB. It is important to note that this relaxation process can be observed for all the CB–aerosil samples (see inset of figure 6). The peak is due to molecular fluctuations that are present neither in the bulk LC nor in the pure aerosil; it can be observed only for the composite systems. Since these samples have a high silica density, and because the LC molecules are located (mostly) in the surface layer, the slow relaxation process has to be assigned to the dynamics of molecules in a surface layer on the silica particles in agreement with previous results [10, 11, 14]. At low temperatures the loss peak is rather broad, but with increasing temperature the process becomes narrower. Assuming that the width of the loss peak is due to the distribution of relaxation times, this implies results that the anchoring of the LC molecules to the surface of silica particles becomes more homogeneous with increasing temperature.

From the position of maximum dielectric loss, the relaxation rate f_p is extracted by fitting the Havriliak–Negami model function to the data. In figure 7 the relaxation rate f_p of the observed relaxation process in the homologous CB series is plotted vs. inverse temperature. The relaxation rates estimated for bulk
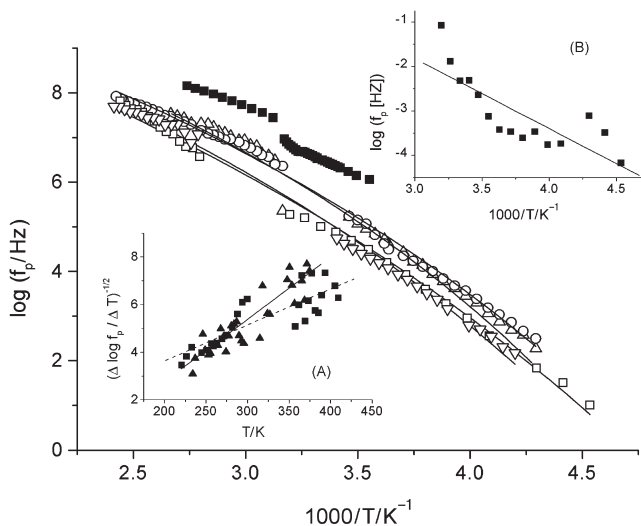
Figure 7. Temperature dependence of the characteristic frequency of the surface layer in composites based on aerosil A_{380} and different CBs: squares = 8CB, down-triangles = 7CB, up-triangles = 6CB, circles = 5CB. The lines are fits of the VFT equation to the data. The solid points are data for bulk 8CB. Inset A gives the differential quotient $(\Delta \log f_p/\Delta T)^{-1/2}$ vs. T for the composites based on 6CB and 8CB; the symbols are the same as in the main figure. The solid line is a linear regression to the data of 6CB; the dashed line is the same for 8CB. The different slopes indicate the different values of T_0. Inset B shows the differential quotient $\Delta \log f_p/\Delta(1/T)$ vs. $1/T$ for a composite based on 8CB in the low frequency region. The line is a linear regression to the data.

Figure 8. Vogel temperature T_0 vs. the number of carbon atoms in the alkyl chain, n; the line is a guide for the eye. The inset presents the temperature dependence of the dielectric strength for the sample 5CB/A_{380} in a temperature interval corresponding to the isotropic bulk. The line is a linear regression to the data.

8CB are also given for comparison. Figure 7 shows that even for temperatures at which the bulk CBs are in the isotropic state, the relaxations estimated for the composites are much lower than for bulk CB. Moreover there is no abrupt change in the temperature dependence of f_p at the transition temperatures of the bulk liquid crystals, indicating that no phase transition takes place in the structure of the surface layer. Also the dielectric strength $\Delta \varepsilon$ varies continuously with temperature, which also supports this conclusion (see inset of figure 8).

At a first glance, the temperature dependence of the relaxation rates seem to follow an Arrhenius equation, but the estimated activation energies are quite high ($E_A \approx 60–65 \, \text{kJ} \, \text{mol}^{-1}$) and the pre-factors are between 10^{15} and 10^{17} Hz. Activations energies in that range are characteristic for the nematic state of the bulk LCs and result from the presence of the nematic potential. In the case of the aerosil composites these high values have to be related to the interaction of CB molecules with the silica surface which also slows down the molecular dynamics. Moreover, a more careful analysis shows
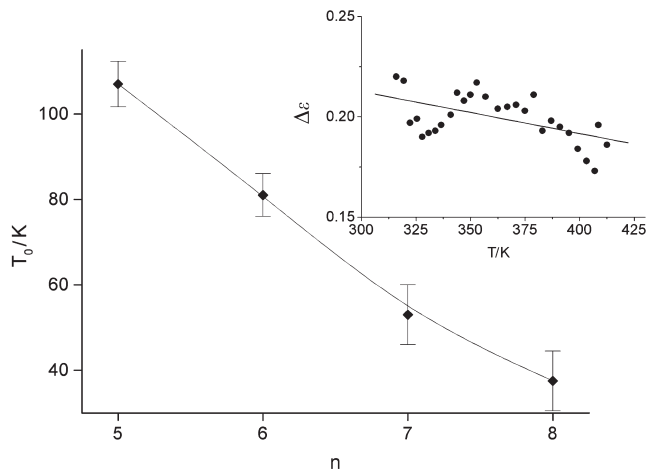
that the relaxation rates follow a curved dependence versus inverse temperature. Although the data show considerable scatter, this is supported by the temperature variation of the difference quotient $(\Delta \log f_p/\Delta T)^{-1/2}$, which decreases linearly with temperature—see inset A, figure 7 and equation (4)—as expected for VFT behaviour. Also the difference quotient $[\Delta \log f_p/\Delta(1/T)]^{-1/2}$ varies with inverse temperature (see inset B, figure 7) but should be constant for an Arrhenius behaviour as follows from equation (5):

$$\frac{d(\log f_p)}{d(1/T)} = -\frac{E_A}{k_B} \log e. \qquad (5)$$

This means that the corresponding molecular motions cannot be characterized by activated processes. The temperature dependence of the relaxation rates can instead be described by the VFT law [22] where realistic values were estimated for the VFT parameters (see the table): f_∞ is comparable with $k_B h/T \sim 6 \times 10^{13}$ Hz (h = Planck's constant). Parameter A has rather high values but can be compared with other values in the literature [12, 25, 26]. T_0 is low, but close to other data on (chemically modified) aerosil composites [12].

Figure 5 gives the relaxation rates of the surface layer as a function of the alkyl chain length at the nematic-to-isotropic transition temperature of the corresponding bulk LC, which were calculated using the estimated VFT parameters. The relaxation rates of the CBs in the composites show no odd–even effect as the bulk, but a continuous decrease with increasing number of carbon

atoms. A reasonable explanation of the disappearance of the odd–even effect might be the changes of the molecular configuration due to strong anchoring to the surface, which fixes the rigid part of the molecules. In addition, these relaxation times are spread over a frequency interval larger than for the corresponding bulk LCs, indicating again that the molecular fluctuations of the molecules in the surface layer are quite different from those in the bulk state.

At temperatures lower than 290 K, the sequence of the relaxation rates follow the order: $5CB/A_{380} > 6CB/A_{380} > 7CB/A_{380} \approx 8CB/A_{380}$; the behaviour of $8CB/A_{380}$ becomes similar to that of $7CB/A_{380}$. Moreover, at even lower temperatures an inversion of the order of the relaxation rates $8CB/A_{380} > 7CB/A_{380}$ (see figure 7) appears, which is in agreement with the dependence of T_0 on the number of carbon atoms in the alkyl chain (see figure 8).

In general it is well accepted that a temperature dependence according to the VFT equation is a characteristic feature for glass-like dynamics. Therefore it is concluded that the molecular dynamics of the surface layer is quite similar to glassy dynamics. This conclusion is supported by the fact that $\Delta\varepsilon$ decreases with increasing temperature (see inset of figure 8). This behaviour is found also to be characteristic for a glass transition [34, 35]. For relaxation processes due to localized molecular fluctuations, usually the dielectric relaxation strength increases with increasing temperature [34]. Because it was argued that the CB molecules form a surface layer on the silica with a nearly monolayer structure, the investigated composites can be regarded as model systems with which to study glass transitions in a quasi two-dimensional system.

The parameters A and T_0 become important at low temperatures. According to the A values, the composites can be arranged in the order: $5CB/A_{380} < 6CB/A_{380} < 7CB/A_{380} < 8CB/A_{380}$. In the framework of the free volume theory, the parameter A can be related to a minimum free volume, which allows molecules to fluctuate. According to these considerations this minimum free volume decreases with increasing length of the alkyl chain, or equivalently the available free volume increases. Figure 8 shows that T_0 increases systematically with decreasing length of the alkyl chain. Generally T_0 is found to be about 50 to 70 K below the glass transition temperature T_g of a glass-forming system. This means that the glass transition temperature of the surface layer also decreases with increasing length of the alkyl chain. A similar behaviour was found for the dependence of the glass transition temperature on the length of the alkyl chain of poly(*n*-alkyl methacrylates) [36]. For the latter system this behaviour was explained by an internal

plasticization effect, which is also equivalent to an increase of available free volume, as discussed already.

From the estimated VFT parameters, the fragility D according to Angell [37] can be calculated using,

$$D \log e = \frac{A}{T_0} \qquad (6)$$

and the values are given in the table. Compared with the values calculated for the isotropic state of bulk CBs these values are quite high, indicating a strong glass-forming system. Often D is related to molecular interactions, which are stronger for fragile glass formers but weaker for strong glass-forming materials. The fact that the D values for the composites are quite high compared with those of the isotropic bulk states, supports the idea of a glass transition in a quasi 2D system. It is expected that in a 2D system the interactions are weaker than in a 3D system.

3.4. *Comparison of the surface layer on an aerosil with that inside the pores*

Recently the molecular dynamics of 5CB and 8CB confined inside the pores of molecular sieves of AlMCM-41 type (2 nm pore diameter) [33] was also studied by dielectric spectroscopy. As for the aerosil composites, a low frequency relaxation process was observed which was assigned to the layer of CB molecules inside the pores. The temperature dependence of its relaxation rates shows a VFT behaviour, also indicating glass-like dynamics. The VFT parameters of these systems based on nanoporous molecular sieves are also given in the table. Thus, a comparison of the dynamics of the surface layers on outer and inner surfaces is possible.

Table. VFT parameters of nCB/A_{380} composites ($n = 5–8$) and related systems.

Sample	A/K	T_0/K	$\log f_\infty$	D	Ref.
$5CB/A_{380}$	1216	107.6	12.0	4.9	This work
$6CB/A_{380}$	1718.2	81.7	13.6	9.1	This work
$7CB/A_{380}$	2187	53.6	14.0	17.7	This work
$8CB/A_{380}$	2416	37.5	14.3	28	This work
$8CB/A_{812}$[a]	2128	106	18.8	17.2	[12]
5CB/AlMCM-41	660.5	168.2	10.7	1.7	[33]
8CB/AlMCM-41	822.0	159.2	10.7	2.2	[33]
5CB[b]	285.5	202.1	10	0.6	This work
6CB[b]	168.0	225.6	9.3	0.32	This work
7CB[b]	348.4	193.5	10.3	0.8	[22]
8CB[b,c]	293.5	204.8	10.0	0.6	[21]

[a]Diffusion coefficients of ESR probe in the nematic range of bulk 8CB.
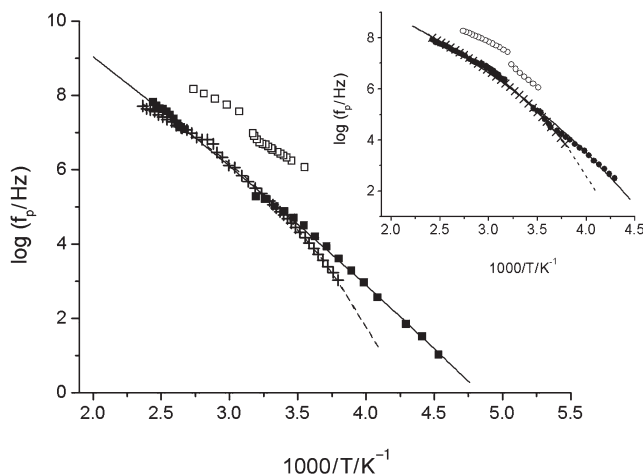[b]In the isotropic phase.
[c]Re-evaluated data.

Figure 9. Relaxation rates vs. inverse temperature for 8CB based systems: open squares bulk state; filed squares 8CB/A$_{380}$; stars 8CB confined to ALMCM. The solid line is a fit of the VFT equation to data for 8CB/A$_{380}$; the dashed line is a fit of the VFT equation to the data for 8CB/AlMCM. The inset shows corresponding results for 5CB.

Figure 9 compares the temperature dependence of the relaxation rates for 8CB in the bulk, the composite 8CB/A$_{380}$ and 8CB confined to AlMCM-41. The inset gives the equivalent data for 5CB. At high temperatures, the relaxation rates of the surface layer of the CB molecules on the aerosil particles have similar temperature dependence as that of the CB molecules inside the cylindrical pores of AlMCM-41. At lower temperatures the relaxation rates of CB molecules confined to nanopores are significantly slower than that of the surface layer on the silica particles. This can be discussed in several ways. Within the pores the molecules are confined in a three-dimensional structure. This causes stronger interaction of the molecules with surfaces (interaction with two surfaces, the pore wall where the molecules are anchored and the opposite pore wall) than with the silica surfaces (interaction with one surface, where the molecules are anchored). On the other hand, the molecules in the pores can have a different orientation (mostly parallel to the surface, due to the confinement) than the molecules on the surfaces of the silica particles (free to orient perpendicular to the surfaces).

4. Conclusions

Composites containing the first cyanobiphenyl liquid crystals in a homologous series and aerosil particles were prepared having a silica density between 7.16 and 7.60 g cm^{-3}. In accordance with previous estimations,

under these conditions the amount of liquid crystal approaches a monolayer with high packing density.

Strong anchoring of the CB molecules at the surface of aerosil particles by hydrogen bonds between the cyano groups of these CB molecules and the hydroxyl groups of the aerosil surface was confirmed by FTIR measurements. Band shape analysis was performed for the broad asymmetrical absorption band observed in the nitrile stretching region: two/three species carrying cyano groups lead to overlapping peaks. Some species form hydrogen bonds with free silanol groups. Other species are sterically hindered to hydrogen bond with the substrate. The integrated intensity of the hydrogen-bonded peak represents the largest part (66–70%) of the asymmetric CN stretch peak for all the composites, indicating that a large fraction of LC molecules are involved in hydrogen bonds.

Homologous cyanobiphenyl molecules in high silica density ($\rho_s \sim 7$ g cm^{-3}) composites containing aerosil particles show a similar dynamical behaviour. A relaxation process was observed which has a much lower relaxation rate than the relaxation processes at lowest frequencies in the corresponding bulk LC. It can also be observed at temperatures were the CB is in the crystalline state and is assigned to a relaxation process of molecules located in a surface layer. The temperature dependence of the relaxation rates was analysed in detail using a derivative technique. It was shown that the temperature dependence of the estimated relaxation rate of the motional process due to the surface layer obeys a VFT law. It is generally believed that such a temperature dependence is a characteristic of glassy dynamics. Therefore it is argued that the investigated composites are model systems with which to study the glass transition in quasi two-dimensional systems.

Relaxation rates of the CBs in composites do not show an odd–even effect, unlike the nematic-to-isotropic transition temperature of the bulk, but a continuous decrease with increasing carbon atom number. Moreover they are spread for all members of the homologous series in the composites over a decade that is 2–3 times larger than the differences observed for the corresponding bulk CBs. The relaxation rate frequencies of the relaxation process (at temperatures corresponding to the crystalline state of bulk LC, $T < 285$ K) follow the sequence 5CB/A$_{380}$ > 6CB/A$_{380}$ > 7CB/A$_{380}$ ≈ 8CB/A$_{380}$ which is discussed within the framework of a free volume approach or equivalently as internal plasticization.

The dynamical behaviour characteristic of glass-forming liquids was compared with that of the surface layer of 5CB and 8CB molecules confined inside the pores (2 nm diameter) of molecular sieves of AlMCM-41 type. At high temperatures, the dynamics are similar

for the surface layer on aerosil particles and inside the pores. At low temperatures, the dynamics become faster on the aerosil than inside the pores. Molecules in the surface layer of silica particles experience weaker interactions than do the LCs confined in the AlMCM-41 cylindrical pores.

References

[1] CRAWFORD, G. P., and ZUMER, S. (editors), 1996, *Liquid Crystals in Complex Geometries Formed by Polymer and Porous Networks* (London:Taylor & Francis), and references therein.

[2] EIDENSCHINK, R., and DE JEU, W. H., 1991, *Electron. Lett.*, **27**, 1195; KREUTZER, M., TSCHUDI, T., DE JEU W. H, and EIDENSCHINK, R., 1993, *Appl. Phys. Lett.*, **62**, 1712.

[3] GLUSHCHENKO, A., KRESSE, H., RESHETNYAK, V., and REZNIKOV, YU, 1997, *Liq. Cryst.*, **23**, 241; HAUSER, A., YAROSHCHUK, O. and KRESSE, H., 1998, *Mol. Cryst. liq. Cryst.*, **324**, 51; ABD-EL-MESSIEH S. L., WERNER, J., SCHMALFUSS, H., WEISSFLOG, W., and KRESSE, H., 1999, *Liq. Cryst.*, **26, 535**.

[4] JAKLI, A., ALMASY, L., BORBELY, S., and ROSTA, L., 1999, *Eur. Phys. J. B*, **10**, 509.

[5] ZHOU, B., IANNACCHIONE, G. S., GARLAND, C. W., and BELLINI, T., 1997, *Phys. Rev. E*, **55**, 2962; ZHOU, B., IANNACCHIONE G. S., and GARLAND, C. W., 1997, *Liq. Cryst.*, **22**, 335.

[6] IANNACCHIONE, G. S., GARLAND, C. W., MANG, J. T., and RIEKER, T. P., 1998, *Phys. Rev. E*, **58**, 5966.

[7] MERCURI, F., GOSH, A. K., and MARINELLI, M., 1999, *Phys. Rev. E*, **60**, R6309; MARINELLI, M., Gosh A. K., and MERCURI, F., 2001, *Phys. Rev. E*, **63**, 061 713.

[8] BELLINI, T., CLARK, N. A., DIGIROGIO, V., MANTEGAZZA, F., and NATALE, G., 1998, *Phys. Rev. E*, **57**, 2996; BELLINI, T., BUSCAGLIA, M., CHICCOLI, C., MANTEGAZZA, F., PASINI, P., and ZANNONI, C., 2000, *Phys. Rev. Lett.*, **85**, 1008.

[9] JIN, T., and FINOTELLO, D., 2001, *Phys. Rev. Lett.*, **86**, 818.

[10] HOURRI, A., BOSE, T. K., and THOEN, J., 2001, *Phys. Rev. E*, **63**, 0 517 706; JAMEE, P., and THOEN, J., 2002, *Phys. Rev. E* **66**, 021 707.

[11] HOURRI, A., JAMEE, P., BOSE, T. K., and THOEN, J., 2002, *Liq. Cryst.*, **29**, 459.

[12] ARCIONI, A., BACCHIOCCHI, C., GROSSI, L., NICOLINI, A., and ZANNONI, C., 2002, *J. phys. Chem. B*, **106**, 9245.

[13] HAGA, H., and GARLAND, C. W., 1997, *Liq. Cryst.*, **23**, 645; HAGA, H., and GARLAND C. W., 1997, *Phys. Rev. E*, **56**, 3044.

[14] FRUNZA, S., FRUNZA, L., GOERING, H., STURM, H., and SCHÖNHALS, A., 2001, *Europhys. Lett.*, **56**, 801.

[15] SCHÖNHALS, A., KREMER, F., and SCHLOSSER, E., 1991, *Phys. Rev. Lett.*, **67**, 999.

[16] SCHLOSSER, E., and SCHÖNHALS, A., 1989, *Colloid polym. Sci.*, **267**, 963.

[17] FRUNZA, L., KOSSLICK, H., BENTRUP, U., PITSCH, I., FRICKE, R., FRUNZA, S., and SCHÖNHALS, A., 2003, *J. mol. Struct.*, **651–653**, 341.

[18] MUELLER, R., KAMMLER, H. K., WEGNER, K., and PRATSINIS, S. E., 2003, *Langmuir*, **19**, 160.

[19] KREUL, H. G., URBAN, S., and WÜRFLINGER, A., 1992, *Phys. Rev. A*, **45**, 8624; BRÜCKERT, T., WÜRFLINGER, A., and URBAN, S., 1993, *Ber. Bunsenges. phys. Chem.* **97**, 1209; URBAN, S., BRÜCKERT, T., and WÜRFLINGER, A., 1994, *Z. Naturforsch.*, **49a**, 552; URBAN, S., GESTBLOM, B., KRESE, H., and DABROWSKI, A., 1996, *Z. Naturforsch.*, **51a**, 834.

[20] ROZANSKI, S. A., STANNARIUS, R., GORBATSCHOW, W., and KREMER, F., 1996, *Liq. Cryst.*, **20**, 59.

[21] SCHÖNHALS, A., ZUBOWA, H.-L., FRICKE, R., FRUNZA, S., FRUNZA, L., and MOLDOVAN, R., 1999, *Cryst. Res. Technol.*, **34**, 1309.

[22] KREMER, F., and SCHÖNHALS, A., 2003, in *Broadband Dielectric Spectroscopy*, edited by F. Kremer and A. Schönhals (Berlin, Heidelberg: Springer-Verlag), pp. 392 ff.

[23] WILLIAMS, G., 1984, in *The Molecular Dyanmics of Liquid Crystals*, edited by G. R. Luckhurst and C. A. Veracini (Dordrecht: Kluwer Academic Press), pp. 431–450.

[24] JADZYN, J., CZECHOWSKI, G., DOUALI, R., and LEGRAND, C., 1999, *Liq. Cryst.*, **26**, 1591.

[25] ZELLER, H. R., 1982, *Phys. Rev. Lett.*, **48**, 334.

[26] BENGUIGUI, L., 1983, *Phys. Rev.*, **A28**, 1852; BENGUIGUI, L., 1984, *Phys. Rev.*, **A29**, 2968; BENGUI-GUI, L., 1984, *Mol. Cryst. liq. Cryst.*, **114**, 51.

[27] DIOGO, A. C., and MARTINS, A. F., 1982, *J. Phys. (Paris)*, **43**, 779.

[28] URBAN, S., GESTBLOM, B., and WÜRFLINGER, A., 1999, *Mol. Cryst. liq. Cryst.*, **331**, 113.

[29] CHANDRASEKHAR, S., 1977, *Liquid Crystals* (Cambridge: Cambridge University Press), pp. 51 ff.

[30] RATNA, B. R., and SHASHIDHAR, R., 1977, *Mol. Cryst. liq. Cryst.*, **42**, 185.

[31] CRAWFORD, G. P., STANNARIUS, R., and DOANE, J. W., 1991, *Phys. Rev. A*, **44**, 2558; CRAWFORD, G. P., ONDRIS-CRAWFORD, R., ZUMER, S., and DOANE, J. W., 1993, *Phys. Rev. Lett.*, **70**, 1838.

[32] SINHA, G. P., and ALIEV, F. M., 1998, *Phys. Rev. E*, **58**, 2001.

[33] FRUNZA, S., SCHÖNHALS, A., FRUNZA, L., ZUBOWA, H.-L., KOSSLICK, H., FRICKE, R., and CARIUS, H., 1999, *Chem. Phys. Lett.*, **307**, 167; FRUNZA, S. FRUNZA, L., and SCHÖNHALS, A., 2000, *J. Phys. IV, Fr.*, **10**, Pr7–115.

[34] SCHÖNHALS, A., 2001, *Europhys. Lett.*, **56**, 815.

[35] SCHÖNHALS, A., 2003, in *Broadband Dielectric Spectroscopy*, edited by F. Kremer and A. Schönhals (Berlin, Heidelberg: Springer-Verlag), pp. 225 ff.

[36] HEIJBOER, J., 1965, in *Physics of Non-Crystalline Solids*, edited by J. A. Prince (Amsterdam: North-Holland) p. 231.

[37] RIECHERT, R., and ANGELL, C. A., 1998, *J. chem. Phys.*, **108**, 9016.